Modeling of Ferroelectric, Semiconducting and Superconducting Perovskite Oxides Using Crystalline Accommodation Law

Tarek El Ashram [1], Eman Elesh [1], Zeinab Mohammed [1], Ansam Gaber [1,*]

[1] Physics Department, College of Science, Port Said University, Port Said, Egypt

* Correspondence author: ansamgaber@sci.psu.edu.eg

―――

ABSTRACT

Perovskite oxides are very important materials for different applications because they have a variety of very interesting properties such as ferroelectric, antiferroelectric, ferromagnetic, antiferromagnetic, semiconducting and superconducting at low temperature. Since the success of crystalline accommodation law (CAL) in modeling perovskite halides, we aim in this work to use CAL for modeling perovskite oxides. Here we show that a perfect agreement with the results obtained for halides perovskite as the following: all perovskite oxides are formed at VEC = 4.8 and most of them crystallize in three systems; cubic, hexagonal and orthorhombic with the number of filled zones in the valence band $(\frac{V_F}{V_B}) = 12, 24$ and 48 respectively. It is also found that the dielectric ferroelectric perovskite oxides have the orthorhombic structure of primitive cell volume (V_P) ranges from 143.58 to 286.93 Å^3 corresponding to the volume of Brillouin zone (V_B, volume of quantum state) ranges from 0.86 to 1.72 Å^{-3}. On average, this is the smallest volume of quantum state. In the case of perovskite oxides, that can be converted into superconductor at low temperature, have cubic structure with V_P ranges from 52.73 to 68.61 Å^3 corresponding to V_B ranges from 3.61 to 4.70 Å^{-3}. On average, this is the largest volume of quantum state for example the compound $SrTiO_3$. In between it is found that the compounds which have hexagonal structure are semiconducting with V_P ranges from 108.73 to 130.43 Å^3 corresponding to V_B ranges from 1.90 to 2.28 Å^{-3}. On the average, this is intermediate between orthorhombic and cubic.

Key Words: Perovskite oxides, Brillouin zone, Valence electron concentration, Crystalline accommodation law, Volume of quantum state.

―――

1. INTRODUCTION

Perovskite oxides (PO) are very important materials for different applications because they have a variety of very interesting properties such as ferroelectric, antiferroelectric, ferromagnetic, antiferromagnetic, semiconducting and superconducting at low temperature [1–6]. Lev Aleksevich Von Perovski, a Russian aristocrat and mineralogist, was honored with initially discovering the calcium titanium oxide ($CaTiO_3$) structure in the Ural Mountains of Russia in 1839, which gave rise to the term "perovskites" [7]. Perovskites are classified into different types and one of its important classifications is PO's. The general chemical formula for PO is ABO_3, in which O is oxygen anion that forms bonds with both A and B, two cations that are very dissimilar in size [8]. All these details are illustrated in Fig. 1, which shows the structure of

PO that is characterized by an octahedral structure. The combination of B cations lie at the center of octahedral and an oxygen anion O^{-2} at the heads of octahedron [9].

For examples the compound $BaTiO_3$ used in supercapacitors [10], $LaFeO_3$ used in gas sensors, and fuel cells [11], $PbTiO_3$ used in nonvolatile memory, infrared sensor, ultrasonic sensor and etc [12].
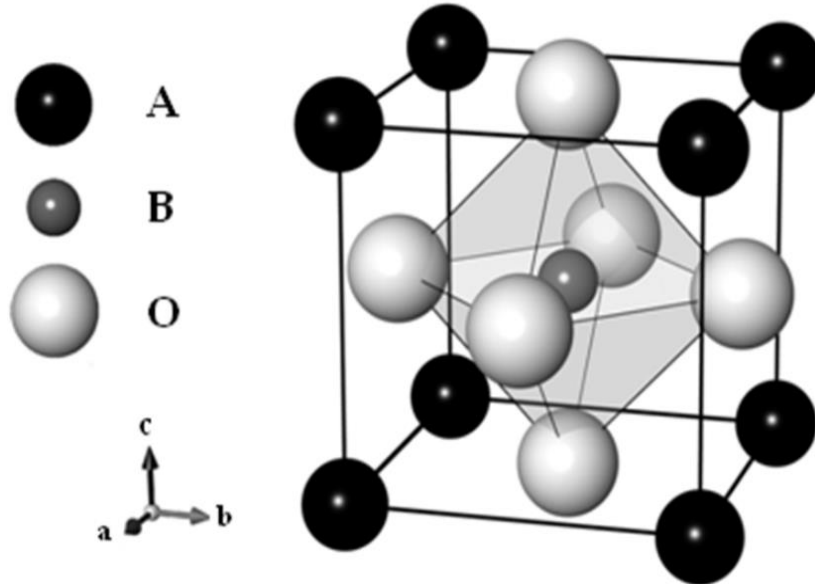

Fig. 1 : Crystal structure of perovskite oxides [13].

There are several attempts have been made to explain the structure of PO by analyzing the size ratio and the geometry of the ions distribution. Goldschmidt attempted to determine the tolerance factor t in 1927 [14] depending on the ionic radius (r) which is given by the following equation;

$$t = \frac{r_A + r_O}{\sqrt{2}(r_B + r_O)} \tag{1}$$

where r_A, r_B and r_O are ionic radii of A, B cations and O anion respectively. This model depends on three probably possible predictions of t values as following; i- the predicted structure is cubic if t equal 1. ii- if t value fall in range $0.825 < t \leq 1.059$, the structure will be either orthorhombic, tetragonal or cubic and iii- in case of t is greater than 1.059, the structure will be hexagonal. If t is lower than 0.825, it will not be crystallized in perovskite structure [14]–[17]. After 47 years exactly in 1974, Muller and Roy [18] assumed the structure of 197 perovskite compounds depending on the ionic radii of cations A and B of PO. They made a structural map between r_A and r_B of 197 PO in structural map and they found that PO where in region away from non-perovskites compounds. However, this model lack of data accuracy of some compounds. In 2001, An octahedral factor µ was proposed by Rohere [19] as given by equation 2;

$$\mu = {r_B}/{r_O} \tag{2}$$

where r_B and r_O are ionic radius of B cation and O oxygen anion atom respectively. Rohere found that the structure of PO is stable when µ value larger than 0.414 and lower than 0.732. Li et al. [20] in 2003 created a t-µ 2D structure map model, which was based on the previous two models developed by Goldschmidt and Rohere. They investigated 64 PO using the structural map. They found that 63 PO follow the structural map and only one compound not follows the structural map. This model is still limited and cannot determine the exact crystal structure of PO. L.Q. Jiange et al. [21] in 2006 tried to predict the lattice constant in the ideal cubic structures of PO using 77 PO have cubic structure. They found that the lattice parameters of all these compounds with average error not exceed 0.63% according to the following equation:

$$a = 1.8836(r_B + r_O) + 1.4898 \frac{(r_A + r_O)}{\sqrt{2}(r_B + r_O)} - 1.2062 \tag{3}$$

where r_A, r_B and r_O are ionic radii of A and B cations and O^{-2} anion respectively. However, some numbers in this equation do not have any physical interpretation and this equation was applied only for cubic PO. Recently in 2019, a modification of t to new tolerance factor τ was applied by Christopher J. Bartel et al. [22] to predict the formation of PO. The new tolerance factor τ is given by;

$$\tau = \frac{r_O}{r_B} - n_A \left(n_A - \frac{r_A/r_B}{\ln(r_A/r_B)} \right) \tag{4}$$

where n_A is the oxidation state of atom A. This study increased the correction possibility of producing perovskite compounds from 83% of Goldschmidt's model to be 92% in this model.

All the previous models are geometrical empirical and have no theoretical basis. In 2017, crystalline accommodation law (CAL) was introduced by Tarek El Ashram [23] and succeeded in explanation the crystalline structure of materials. Moreover a very important model, based on CAL, was obtained by Tarek El Ashram [24] called the quantum quantitative model (CALQQM). CALQQM is succeeded in explaining the superconductivity at room temperature, energy levels, and the work functions of materials. In addition CAL is succeeded in modeling inorganic perovskite halides (PH) and determined the electronic structures of their valence bands [25]. Since the success of crystalline accommodation law in modeling PH's, we aim in this work to use CAL for modeling PO's.

2. COMPUTATIONAL METHODOLOGY

The computational methodology was based on CAL. The parameters of CAL are *VEC, n, V_F* and *V_B*. These parameters were calculated from the crystal structure data obtained from ICDD cards [26] shown in Table 1 as the following;

1- **VEC** *is given by;*

$$VEC = \frac{VEC \text{ of } A + VEC \text{ of } B + VEC \text{ of } O}{5} \tag{5}$$

The PO molecule consists of five atoms, 2 cations A and B and 3 anions O. According to the charge neutrality of the molecule, the charge on cations must equal to the charge on the anions. The charge on the cations varies in three different forms as the following; $A^{+3}B^{+3}O_3$ such as $GdGaO_3$, $A^{+2}B^{+4}O_3$ such as $CaTiO_3$ and $A^{+1}B^{+5}O_3$ such as $KTaO_3$. For examples;

For $GdGaO_3$ $VEC = \frac{1*3+1*3+3*6}{5} = 4.8$, $CaTiO_3$ $VEC = \frac{1*2+1*4+3*6}{5} = 4.8$ and for $KTaO_3$

$VEC = \frac{1*1+1*5+3*6}{5} = 4.8$. Actually it was found that all PO and PH are formed at VEC = 4.8.

2- **n** is the number of atoms per lattice point calculated from diffraction data shown on Table 1.

3- **V_F** is the volume of Fermi sphere and determined by;

$$V_F = \frac{4}{3}\pi K_F^3 \tag{6}$$

where **K_F** is the Fermi electron wave vector given by;

$$K_F^3 = \frac{3\pi^2(0.6022)n \, VEC \, Dx}{Mwt} \tag{7}$$

where *Mwt* is the molecular weight and *Dx* is the calculated density from X-ray diffraction data

4- **V_B** is the volume of Brillouin zone (BZ) which is the volume of quantum state and is given by;

$$V_B = \frac{8\pi^3}{V_P} \qquad (8)$$

where V_P is the primitive cell volume.

The calculations were carried out on the PO, which are stable in normal conditions of temperature and pressure as shown in Table 1.

3. RESULTS AND DISCUSSION

The parameters of CAL for PO's were calculated as given in Table 2. It is evident that all of PO's are formed at the same VEC = 4.8 in agreement with the results obtained for PH's [25]. It also found that PO's crystallize in three main systems, cubic, hexagonal and orthorhombic. For cubic system it was found that the number of filled zones in the valence band $(\frac{V_F}{V_B}) = 12$. For the hexagonal system it was found that the number of filled zones in the valence band $(\frac{V_F}{V_B}) = 24$. For the orthorhombic system it was found the number of filled zones in the valence band $(\frac{V_F}{V_B}) = 48$ in agreement with the results obtained for PH's [25].
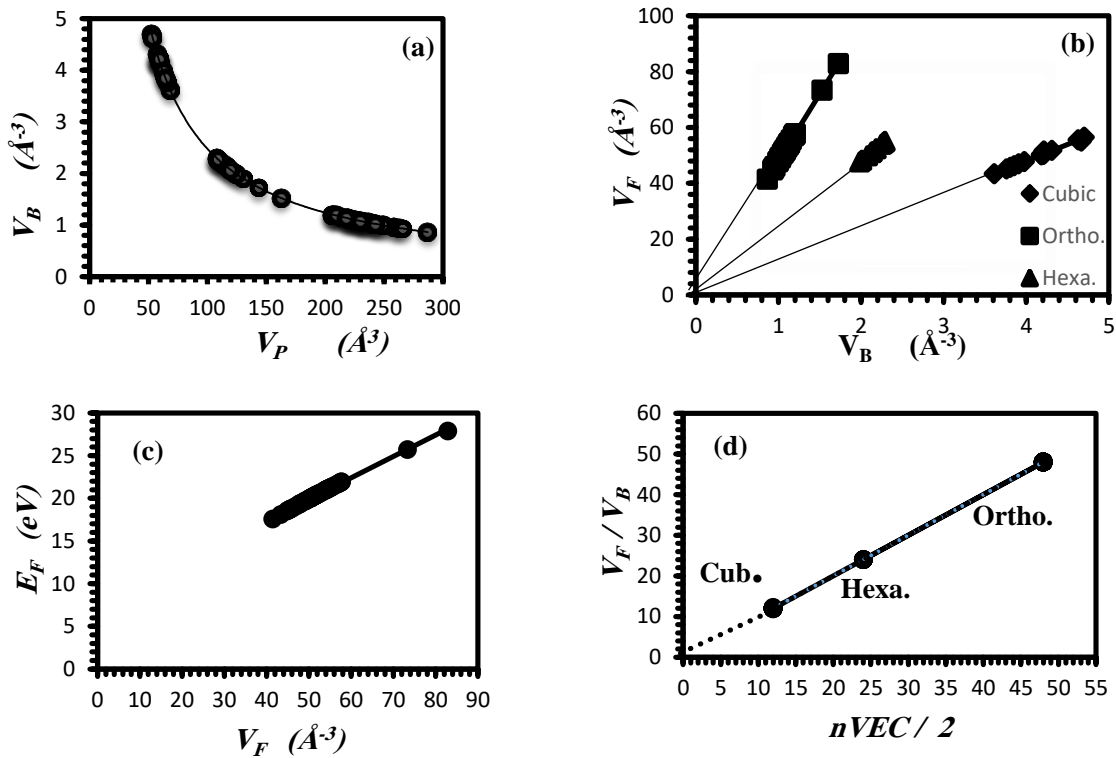

Fig. 2: (a) Variation of BZ volume with the primitive cell volume. (b) Variation of Fermi sphere volume with BZ volume. (c) Variation of Fermi energy with Fermi sphere volume. (d) Verification of CAL for PO's.

Fig. 2a. shows the variation of V_B with V_P. It shows that V_B decreases by increasing V_P as predicted by equation (8). This means that the volume of quantum state decreases by incresing V_P. The maximum volume of quantum state was found to be $V_B = 4.70767 \text{ Å}^{-3}$ for $SmCoO_3$ and the minimum volume of quantum state was found to be $V_B = 0.864487 \text{ Å}^{-3}$ for $PrLuO_3$. This result indicates that $SmCoO_3$ can be converted into superconductor at low temperature while $PrLuO_3$ is dielectric [6]. It was also found that for PO's, that have the orthorhombic structure, V_P ranges from 143.5876 to 286.9334 Å^3 corresponding to V_B ranges from 0.864487 to 1.72751 Å^{-3}. On the average, this is the smallest volume of quantum state. In case of PO's with cubic structure, V_P ranges from 52.73438 to 68.61886 Å^3 corresponding to the volume V_B ranges from 3.614898 to 4.703767 Å^{-3}. On the average, this is the largest volume of quantum state. In

between we found that PO's, that have hexagonal structure, have V_P ranges from 108.7328 to 130.4333 $Å^3$ corresponding to V_B ranges from 1.90174 to 2.281282 $Å^{-3}$.

Fig. 2b. shows the variation of V_F with V_B. It shows that V_F increases linearly with V_B according to CAL for the three crystalline systems (cubic, hexagonal and orthorhmbic). The maximum V_F was found for orthorhmbic system $V_F = 82.9195$ $Å^{-3}$ for $PbZrO_3$, and the minimum was found for distorted cubic system $V_F = 34.59461$ $Å^{-3}$ for $BaBiO_3$. Fig. 2c shows the variation of E_F with V_F. It shows that E_F increases by increasing V_F from 15.567 eV up to maximum value 27.8807 eV for $PbZrO_3$ orthorhombic compound. The minimum value of E_F was found to be 15.567 eV for $BaBiO_3$ distorted cubic. On the average E_F is greater for orthorhmbic system than hexagonal system and is small for cubic system.

Fig. 2d shows the relation between V_F/V_B and nVEC/2. It shows that a linear relation as predicted by CAL. That means verification of CAL for PO's.

The PO's that can be converted into superconductors at low temperature have cubic structure with the largest volume of quantum state as $SrTiO_3$. This compound is the most famous compound to have superconducting properties [27]. The dielectric PO's have the orthorhombic structure with the smallest volume of quantum state. It is found that the PO's with hexagonal structure are semiconducting and have intermediate volume of quantum state such as $BaCoO_3$. It is clear from the above results that the electrical properties of PO's depend on the volume of quantum states. The connection between the electrical properties and the volume of quantum state is in a good agreement with CALQQM results [24].

Table 1 : Crystal structure data obtained from ICDD cards [26] for PO's used in this study.

compound	card no.	System	S.G	Z	VEC	n	Dx (gm/cm³)	Mwt (gm/mol)	a (Å)	b (Å)	c (Å)
CeCrO₃	750289	Cub.	Pm3⁻m	1	4.8	5	6.774	240.11	3.89		
PrCoO₃	750280	Cub	Pm3⁻m	1	4.8	5	7.62	247.84	3.76		
SmCoO₃	750282	Cub	Pm3⁻m	1	4.8	5	8.103	257.33	3.75		
SrNbO₃	790625	Cub	Pm3⁻m	1	4.8	5	5.824	228.52	4.024		
KTaO₃	770918	Cub	Pm3⁻m	1	4.8	5	7.016	268.04	3.9883		
NdCoO₃	750281	Cub	Pm3⁻m	1	4.8	5	7.784	251.17	3.77		
SrTiO₃	840443	Cub	Pm3⁻m	1	4.8	5	5.145	183.52	3.898		
SrZrO₃	760167	Cub	Pm3⁻m	1	4.8	5	5.489	226.84	4.094		
CeVO₃	750284	Cub	Pm3⁻m	1	4.8	5	6.692	239.06	3.9		
NdVO₃	750286	Cub	Pm3⁻m	1	4.8	5	6.86	243.18	3.89		
PrCrO₃	750290	Cub	Pm3⁻m	1	4.8	5	6.796	240.9	3.89		
PrVO₃	750285	Cub	Pm3⁻m	1	4.8	5	6.766	239.85	3.89		
SmCrO₃	750292	Cub	Pm3⁻m	1	4.8	5	7.23	250.39	3.86		
SmVO₃	750287	Cub	Pm3⁻m	1	4.8	5	7.034	244.34	3.89		
SrMoO₃	810640	Cub	Pm3⁻m	1	4.8	5	6.168	231.56	3.9651		
BaMoO₃	893139	Cub	Pm3⁻m	1	4.8	5	7.081	281.27	4.0404		
BaTiO₃	831880	Distorted cub.	P4mm	1	4.8	5	6.018	233.23	3.9945		4.0335
BaBiO3	700602	Distorted cub.	P4⁻2m	1	4.8	5	7.61	394.31	4.364		4.518
PbTiO3	780299	Distorted cub.	P4mm	1	4.8	5	7.98	303.1	3.94		4.063
CdTiO₃	781015	ortho	Pbn21	4	4.8	20	6.315	208.31	5.3063	5.4215	7.6176
NdGaO₃	812294	ortho	Pbn21	4	4.8	20	7.571	261.96	5.4243	5.5014	7.7016
CaZrO₃	762401	ortho	Pcmn	4	4.8	20	4.611	179.3	5.5912	8.0171	5.7616
NdCrO₃	880472	ortho	Pnma	4	4.8	20	7.098	244.23	5.4798	7.6918	5.4221
NdFeO₃	886644	ortho	Pnma	4	4.8	20	6.971	248.09	5.5887	7.7619	5.4489
CaVO₃	860358	ortho	Pnma	4	4.8	20	4.312	139.02	5.3171	7.5418	5.3396
SrRuO₃	895713	ortho	Pnma	4	4.8	20	6.488	236.69	5.5368	7.8523	5.5731
LaCrO₃	831327	ortho	Pnma	4	4.8	20	6.782	238.9	5.476	7.752	5.512
PrLuO₃	894507	ortho	Pnma	4	4.8	20	8.423	363.87	5.9868	8.3202	5.7604
LaTiO₃	841089	ortho	Pbnm	4	4.8	20	6.246	234.8	5.6247	5.6071	7.9175
CaSnO₃	771797	ortho	Pbnm	4	4.8	20	5.527	206.77	5.532	5.681	7.906
CaTiO₃	820232	ortho	Pbnm	4	4.8	20	3.876	135.98	5.475	5.4863	7.7579
CaGeO₃	751764	ortho	Pbnm	4	4.8	20	5.171	160.67	5.2607	5.2688	7.4452
DyCoO₃	731197	ortho	Pbnm	4	4.8	20	8.678	269.43	5.162	5.4	7.398
HoCoO₃	731198	ortho	Pbnm	4	4.8	20	8.719	271.86	5.157	5.429	7.397
TbCoO₃	731196	ortho	Pbnm	4	4.8	20	8.484	265.86	5.2	5.394	7.421
LaVO₃	782305	ortho	Pbnm	4	4.8	20	6.558	237.85	5.543	5.543	7.84
MgSiO₃	841289	ortho	Pbnm	4	4.8	20	4.107	100.39	4.7754	4.9292	6.8969
YFeO₃	892609	ortho	Pbnm	4	4.8	20	5.696	192.75	5.2819	5.5956	7.6046
SrSnO₃	771798	ortho	Pbnm	4	4.8	20	6.431	254.31	5.707	5.707	8.064
GdGaO₃	700238	ortho	Pbnm	4	4.8	20	8.098	274.97	5.334	5.548	7.621
TbMnO₃	720379	ortho	Pbnm	4	4.8	20	7.607	261.86	5.297	5.831	7.403
PrRhO₃	231388	ortho	Pbnm	4	4.8	20	7.983	291.81	5.4143	5.7473	7.8026
SmAlO₃	711597	ortho	Pbnm	4	4.8	20	7.155	225.38	5.2912	5.2904	7.474
SmFeO₃	741474	ortho	Pbnm	4	4.8	20	7.246	254.25	5.4	5.597	7.711
SmInO₃	251106	ortho	Pbnm	4	4.8	20	7.825	313.22	5.587	5.875	8.1
SmNiO₃	801948	ortho	Pbnm	4	4.8	20	7.789	257.1	5.3283	5.4374	7.5675
TbCrO₃	251072	ortho	Pbnm	4	4.8	20	7.803	258.92	5.288	5.506	7.57
NdNiO₃	801947	ortho	Pbnm	4	4.8	20	7.546	250.94	5.3888	5.3845	7.6127

PrNiO$_3$	801946	ortho	Pbnm	4	4.8	20	7.415	247.61	5.4154	5.3755	7.6192
YCrO$_3$	340365	ortho	Pnma	4	4.8	20	5.751	188.9	5.5237	7.5343	5.2427
GdFeO$_3$	780451	ortho	Pnma	4	4.8	20	7.533	261.1	5.616	7.668	5.346
PbZrO$_3$	770856	ortho	Pbma	4	4.8	20	16.025	346.42	5.89	5.897	4.134
YBO$_3$	880356	Hexa	P63/m	2	4.8	10	4.512	147.71	3.776		8.806
YAlO$_3$	741334	Hexa	P63/mmc	2	4.8	10	4.411	163.89	3.68		10.52
InFeO$_3$	852306	Hexa	P63/mmc	2	4.8	10	6.222	218.67	3.327		12.175
BaCoO$_3$	740902	Hexa	P63/mmc	2	4.8	10	6.219	244.26	5.59		4.82
DyBO$_3$	741933	Hexa	P63/mmc	2	4.8	10	6.668	221.31	3.793		8.847
ErBO$_3$	741935	Hexa	P63/mmc	2	4.8	10	6.937	226.07	3.767		8.807
GdBO$_3$	741932	Hexa	P63/mmc	2	4.8	10	6.312	216.06	3.839		8.906
HoBO$_3$	741934	Hexa	P63/mmc	2	4.8	10	6.782	223.74	3.784		8.836
SmBO$_3$	741930	Hexa	P63/mmc	2	4.8	10	5.991	209.21	3.862		8.978
BiFeO$_3$	712494	Roh-Hex	R3c	6	4.8	10	8.313	312.83	5.5876		13.867
LaAlO$_3$	851071	Roh-Hex	R3⁻m	6	4.8	10	6.52	213.89	5.3651		13.11199
LaCoO$_3$	861665	Roh-Hex	R3⁻m	6	4.8	10	6.838	245.84	5.5397		13.47863

Table 2: Results of CAL parameters for PO's.

Compound	*System*	*V_P (Å^3)*	*V_B (Å^{-3})*	*E_F(eV)*	*V_F (Å^{-3})*	*nVEC/2*	*V_F/V_B*
CeCrO$_3$	Cub	58.86387	4.213964	20.05073	50.57042	12	12.00068
PrCoO$_3$	Cub	53.15738	4.666337	21.23388	55.11187	12	11.81052
SmCoO$_3$	Cub	52.73438	4.703767	21.57466	56.4439	12	11.99972
SrNbO$_3$	Cub	65.15893	3.806849	18.73722	45.68344	12	12.00033
KTaO$_3$	Cub	63.44004	3.909995	19.07364	46.91931	12	11.99984
NdCoO$_3$	Cub	53.58263	4.629302	21.34668	55.55161	12	12
SrTiO$_3$	Cub	59.22779	4.188072	19.96679	50.25318	12	11.99912
SrZrO$_3$	Cub	68.61886	3.614898	18.10045	43.37457	12	11.99884
CeVO$_3$	Cub	59.319	4.181632	19.94679	50.17768	12	11.99955
NdVO$_3$	Cub	58.86387	4.213964	20.04954	50.56591	12	11.99961
PrCrO$_3$	Cub	58.86387	4.213964	20.05017	50.56828	12	12.00017
PrVO$_3$	Cub	58.86387	4.213964	20.04942	50.56545	12	11.9995
SmCrO$_3$	Cub	57.51246	4.312982	20.3636	51.75865	12	12.00066
SmVO$_3$	Cub	58.86387	4.213964	20.32258	51.60234	12	12.24556
SrMoO$_3$	Cub	62.33937	3.97903	19.2972	47.7466	12	11.99956
BaMoO$_3$	Cub	65.95885	3.760681	18.58465	45.12662	12	11.99959
BaTiO$_3$	Distorted cub.	64.3587	3.854186	18.89233	46.25188	12	12.00043
BaBiO3	Distorted cub.	86.043	2.882862	15.567	34.59461	12	12.00009
PbTiO3	Distorted cub.	63.0724	3.932786	19.14777	47.19311	12	11.99992
CdTiO$_3$	ortho	219.1439	1.131906	21.03532	54.34065	48	48.00812
NdGaO$_3$	ortho	229.8253	1.079299	20.37601	51.80598	48	47.99966
CaZrO$_3$	ortho	258.2649	0.960449	18.85024	46.0974	48	47.99569
NdCrO$_3$	ortho	228.5389	1.085374	20.4518	52.09531	48	47.99756
NdFeO$_3$	ortho	236.3675	1.049426	19.99697	50.36716	48	47.99495
CaVO$_3$	ortho	214.1207	1.15846	21.35869	55.5985	48	47.99346
SrRuO$_3$	ortho	242.2995	1.023734	19.66954	49.13518	48	47.99605
LaCrO$_3$	ortho	233.9841	1.060116	20.13422	50.88658	48	48.00097
PrLuO$_3$	ortho	286.9334	0.864487	17.57333	41.4937	48	47.99806
LaTiO$_3$	ortho	249.7041	0.993376	19.28011	47.68321	48	48.00115

CaSnO$_3$	ortho	248.4642	0.998334	19.34231	47.91412	48	47.99408
CaTiO$_3$	ortho	233.0279	1.064466	20.18891	51.09405	48	47.99971
CaGeO$_3$	ortho	206.3629	1.20201	21.89106	57.69011	48	47.99471
DyCoO$_3$	ortho	206.2178	1.202856	21.90229	57.73449	48	47.99785
HoCoO$_3$	ortho	207.0964	1.197752	21.8401	57.48876	48	47.99721
TbCoO$_3$	ortho	208.1501	1.191689	21.76734	57.20174	48	48.00057
LaVO$_3$	ortho	240.8828	1.029755	19.7463	49.42309	48	47.99501
MgSiO$_3$	ortho	162.3455	1.527916	25.68797	73.33239	48	47.99504
YFeO$_3$	ortho	224.757	1.103637	20.68033	52.97088	48	47.99664
SrSnO$_3$	ortho	262.6433	0.944438	18.64019	45.32906	48	47.99581
GdGaO$_3$	ortho	225.5285	1.099862	20.6333	52.79029	48	47.9972
TbMnO$_3$	ortho	228.655	1.084823	20.44575	52.07219	48	48.00064
PrRhO$_3$	ortho	242.7982	1.021631	19.64344	49.03741	48	47.99914
SmAlO$_3$	ortho	209.2164	1.185615	21.69218	56.90571	48	47.99677
SmFeO$_3$	ortho	233.0557	1.064339	20.18669	51.08566	48	47.99756
SmInO$_3$	ortho	265.8714	0.932971	18.48971	44.78128	48	47.99858
SmNiO$_3$	ortho	219.2464	1.131377	21.02616	54.30518	48	47.9992
TbCrO$_3$	ortho	220.4061	1.125424	20.95259	54.02038	48	48.00003
NdNiO$_3$	ortho	220.8901	1.122958	20.92208	53.90245	48	48.00042
PrNiO$_3$	ortho	221.7986	1.118358	20.86423	53.67902	48	47.99807
YCrO$_3$	ortho	218.1866	1.136872	21.09508	54.57239	48	48.00223
GdFeO$_3$	ortho	230.2174	1.077461	20.35234	51.71573	48	47.99779
PbZrO$_3$	ortho	143.5876	1.727519	27.8807	82.9195	48	47.9992
YBO$_3$	Hexa	108.7328	2.281282	21.14202	54.75462	24	24.00169
YAlO$_3$	Hexa	123.3756	2.010529	19.43107	48.24432	24	23.99584
InFeO$_3$	Hexa	116.7058	2.125432	20.16512	51.00378	24	23.99691
BaCoO$_3$	Hexa	130.4333	1.90174	18.72488	45.63834	24	23.9982
DyBO$_3$	Hexa	110.2249	2.250401	20.94932	54.00776	24	23.99917
ErBO$_3$	Hexa	108.2274	2.291936	21.20604	55.0035	24	23.99871
GdBO$_3$	Hexa	113.6676	2.182241	20.52274	52.36658	24	23.99669
HoBO$_3$	Hexa	109.566	2.263934	21.03374	54.33451	24	24.00004
SmBO$_3$	Hexa	115.9637	2.139033	20.25124	51.33085	24	23.99722
BiFeO$_3$	Roh-Hex	124.9806	1.98471	19.26667	47.63333	24	24.00015
LaAlO$_3$	Roh-Hex	108.9514	2.276705	21.11276	54.64101	24	24.00004
LaCoO$_3$	Roh-Hex	119.4153	2.077207	19.86208	49.85838	24	24.00261

4. REFERENCES

[1] Y. Maeno *et al.*, "Superconductivity in a layered perovskite without copper," *Nature*, vol. 372, no. 6506, pp. 532–534, Dec. 1994, doi: 10.1038/372532a0.

[2] J. Torrance, P. Lacorre, A. Nazzal, E. Ansaldo, and C. Niedermayer, "Systematic study of insulator-metal transitions in perovskites RNiO3 (R=Pr,Nd,Sm,Eu) due to closing of charge-transfer gap," *Phys. Rev. B*, vol. 45, no. 14, pp. 8209–8212, Apr. 1992, doi: 10.1103/PhysRevB.45.8209.

[3] O. Bohnke, "Mechanism of ionic conduction and electrochemical intercalation of lithium into the perovskite lanthanum lithium titanate," *Solid State Ionics*, vol. 91, no. 1–2, pp. 21–31, Oct. 1996, doi: 10.1016/S0167-2738(96)00434-1.

[4] G. A. Samara, "Pressure and temperature dependence of the dielectric properties and phase transitions of the ferroelectric perovskites: PbTiO3 and BaTiO3," *Ferroelectrics*, vol. 2, no. 1, pp. 277–289, Oct. 1971, doi: 10.1080/00150197108234102.

[5] P. P. Khirade and A. V. Raut, "Perovskite Structured Materials: Synthesis, Structure, Physical Properties and Applications," in *Recent Advances in Multifunctional Perovskite Materials*, IntechOpen, 2022. doi: 10.5772/intechopen.106252.

[6] A. A. Demkov and A. B. Posadas, "Integration of Functional Oxides with Semiconductors," *Integr. Funct. Oxides with Semicond.*, pp. 1–278, 2014, doi: 10.1007/978-1-4614-9320-4.

[7] Z. Cheng and J. Lin, "Layered organic–inorganic hybrid perovskites: structure, optical properties, film preparation, patterning and templating engineering," *CrystEngComm*, vol. 12, no. 10, p. 2646, 2010, doi: 10.1039/c001929a.

[8] T. E. Warner, *Synthesis, Properties and Mineralogy of Important Inorganic Materials*. Wiley, 2011. doi: 10.1002/9780470976012.

[9] "Ferroelectric Materials and Their Applications," *Jpn. J. Appl. Phys.*, vol. 55, no. 10S, p. 10T001, Oct. 2016, doi: 10.7567/JJAP.55.10T001.

[10] Z. Ben Cheikh *et al.*, "Hydrogen doped BaTiO3 films as solid-state electrolyte for micro-supercapacitor applications," *J. Alloys Compd.*, vol. 721, pp. 276–284, Oct. 2017, doi: 10.1016/j.jallcom.2017.06.019.

[11] M. Theingi, K. T. Tun, and N. N. Aung, "Preparation, Characterization and Optical Property of LaFeO3 Nanoparticles via Sol-Gel Combustion Method," *SciMedicine J.*, vol. 1, no. 3, pp. 151–157, Sep. 2019, doi: 10.28991/SciMedJ-2019-0103-5.

[12] M. Okuyama and Y. Hamakawa, "Preparation and basic properties of PbTiO 3 ferroelectric thin films and their device applications," *Ferroelectrics*, vol. 63, no. 1, pp. 243–252, Jun. 1985, doi: 10.1080/00150198508221406.

[13] J. A. Onrubia-Calvo, B. Pereda-Ayo, and J. R. González-Velasco, "Perovskite-Based Catalysts as Efficient, Durable, and Economical NOx Storage and Reduction Systems," *Catalysts*, vol. 10, no. 2, p. 208, Feb. 2020, doi: 10.3390/catal10020208.

[14] FRANCIS S. GALASSO, *STRUCTURE, PROPERTIES AND PREPARATION OF PEROVSKITE-*

TYPE COMPOUNDS. 1969.

[15] K. Karthick, S. R. Ede, U. Nithiyanantham, and S. Kundu, "Low-temperature synthesis of SrTiO 3 nanoassemblies on DNA scaffolds and their applications in dye-sensitized solar cells and supercapacitors," *New J. Chem.*, vol. 41, no. 9, pp. 3473–3486, 2017, doi: 10.1039/C7NJ00204A.

[16] A. SMM., "Synthesis of Nano-particles Using Microwave Technique, the Study of their Physical Properties and Some Applications [PhD thesis].," Faculty of Science Cairo University, 2009.

[17] E. S. Wolfram T, *Electronic and Optical Properties of d-band Perovskites.*, 1st ed. Cambridge University Press: New York, 2006.

[18] O. Muller and R. Roy, *The Major Ternary Structural Families*. Berlin, Heidelberg: Springer Berlin Heidelberg, 1974. doi: 10.1007/978-3-642-65706-1.

[19] G. S. Rohrer, *Structure and Bonding in Crystalline Materials*. Cambridge University Press, 2001. doi: 10.1017/CBO9780511816116.

[20] C. Li, K. C. K. Soh, and P. Wu, "Formability of ABO3 perovskites," *J. Alloys Compd.*, vol. 372, no. 1–2, pp. 40–48, Jun. 2004, doi: 10.1016/j.jallcom.2003.10.017.

[21] L. Q. Jiang *et al.*, "Prediction of lattice constant in cubic perovskites," *J. Phys. Chem. Solids*, vol. 67, no. 7, pp. 1531–1536, Jul. 2006, doi: 10.1016/j.jpcs.2006.02.004.

[22] C. J. Bartel *et al.*, "New tolerance factor to predict the stability of perovskite oxides and halides," *Sci. Adv.*, vol. 5, no. 2, Feb. 2019, doi: 10.1126/sciadv.aav0693.

[23] T. El Ashram, "CRYSTALLINE ACCOMMODATION LAW EXPLAINS THE CRYSTALLINE STRUCTURE OF MATERIALS," *J. Adv. Phys.*, pp. 5069–5075, Dec. 2017, doi: 10.24297/jap.v13i8.6295.

[24] T. El Ashram, "Precise Determination of Energy Levels, Work Function and Explanation of Near-Ambient Superconductivity of Solids By Quantum Quantitative Model," *Alfarama J. Basic Appl. Sci.*, pp. 0–0, Sep. 2023, doi: 10.21608/ajbas.2023.227822.1169.

[25] A. Gaber, Z. Mohammed, E. Elesh, and T. El Ashram, "Crystalline Accommodation Law Modeling for the Structure of Inorganic Perovskite Halides Used in Solar Cells," *Alfarama J. Basic Appl. Sci.*, pp. 0–0, Oct. 2023, doi: 10.21608/ajbas.2023.222640.1162.

[26] International Center for Diffraction Data, "PCPDFWIN," vol. PCPDFWIN v, p. PA 19081-2389, 2002.

[27] M. Jourdan, N. Blumer, and H. Adrian, "Superconductivity of SrTiO $\mathsf{_{3-\delta}}$," *Eur. Phys. J. B -Condens. Matter*, vol. 33, no. 1, pp. 25–30, May 2003, doi: 10.1140/epjb/e2003-00137-0.